Journal of Power Sources 210 (2012) 21–25

Contents lists available at SciVerse ScienceDirect

Journal of Power Sources

journal homepage: www.elsevier.com/locate/jpowsour

Short communication

Electrical and electron paramagnetic resonance spectroscopy characterization of Mn-doped nanostructured TiO_2 for capacitor applications

Rafael Vazquez-Reina [a], Sheng Chao [b], Vladimir Petrovsky [b], Fatih Dogan [b], Steven Greenbaum [a,*]

[a] Department of Physics & Astronomy, Hunter College of the City University of New York and Graduate Center of the City University of New York, New York, NY 10065, USA
[b] Department of Materials Science & Engineering, Missouri University of Science and Technology, Rolla, MO 65409, USA

ARTICLE INFO

Article history:
Received 23 January 2012
Received in revised form 21 February 2012
Accepted 23 February 2012
Available online 3 March 2012

Keywords:
Capacitors
Nanostructured TiO_2
Insulation resistance
Electron paramagnetic resonance (EPR)

ABSTRACT

Nanostructured TiO_2 has shown promise as a dielectric material for high energy density ceramic capacitors because of its high dielectric breakdown strength and dielectric constant. Strategies to increase the insulation resistance or to reduce the leakage current of TiO_2 include doping with transition metal ions. It is shown that Mn doping followed by an appropriate thermal treatment increases the grain boundary resistivity significantly and lowers the dielectric loss. Electrical measurements along with electron paramagnetic resonance and scanning electron microscopy of Mn-doped nanoscopic TiO_2 demonstrate that sintering at 900 °C leads to optimal electrical properties that are correlated with a non-uniform distribution of dopant ions, concentrated at the grain boundaries. Nanostructured TiO_2 dielectrics with improved insulation resistance are promising for the development of higher energy density capacitors.

1. Introduction

Energy storage capacitors with reduced volume are increasingly in high demand for military applications in mobile platforms including vehicles, airplanes and ships. The key to the improvement of energy storage capability of a capacitor is to increase the energy density of the dielectric materials occupying most of the volume of a capacitor. Dielectrics with high dielectric constant, breakdown strength and insulation resistance are required for high energy density capacitor applications. Among various types of dielectric materials (ceramics, polymers, composites), ceramics are the mostly widely used ones [1]. Due to the advantages of high dielectric constant, ceramic capacitors can easily achieve high capacitance density. However, high energy density cannot be readily accomplished without high breakdown strength and insulation resistance of the dielectrics. Energy density of multilayer ceramic capacitors (MLCC) are typically <2 J cm^{-3}. There is an increasing interest in higher energy density (>5 J cm^{-3}) MLCCs particularly for pulsed power applications. Previous research showed that nanostructured titanium dioxide (TiO_2) ceramics exhibit significantly higher breakdown strength than conventional microsized TiO_2, making them suitable for energy storage applications [2]. It was also found that the dielectric properties of TiO_2 are greatly affected by impurities (dopants) and defects [3] as well as processing conditions [4]. Earlier studies showed that Mn doping can hinder the reduction of $BaTiO_3$ thereby suppressing one of the dominant defects, oxygen vacancies [5,6]. Application of this method to TiO_2 suggests that optimal amounts of Mn^{2+} suppress the reduction of Ti^{4+} [7].

In order to further clarify the effect of the dopants on the microstructural development and resultant dielectric properties of TiO_2, electron paramagnetic resonance (EPR) spectroscopy was employed in the current study. TiO_2 ceramics doped with manganese were subjected to the EPR analysis and the results were correlated with measurements of dielectric properties.

EPR signals arise from paramagnetic impurities, whether residual or intentional (from doping) or from paramagnetic defects such as dangling bonds. For example, the oxygen vacancy is the predominant defect in TiO_2 and has an associated EPR response [8]. The oxygen deficiency introduces an excess of electrons in the material resulting in an increase of the electrical conductivity and dielectric loss [7], which has a deleterious effect on the material's breakdown strength and insulation resistance. EPR also has been used previously to investigate the nature of paramagnetic impurities in various forms of TiO_2. For example, in studies of photochemical properties of vanadium-doped TiO_2 particles for photooxidation applications both surface VO^{2+} and interstitial V^{4+} species were detected [9]. In another example, EPR was used to investigate the environment of Mn^{4+} ions in Mn-implanted single crystals of TiO_2 rutile [10]. In both of these cases, the hyperfine splitting characteristics of the ^{51}V and ^{55}Mn nuclei, respectively, were clearly observed, indicating that the dopant ions were well dispersed in the host crystal.

* Corresponding author. Tel.: +1 212 772 4973; fax: +1 212 772 5390.
E-mail address: steve.greenbaum@hunter.cuny.edu (S. Greenbaum).

0378-7753/$ – see front matter © 2012 Elsevier B.V. All rights reserved.
doi:10.1016/j.jpowsour.2012.02.096

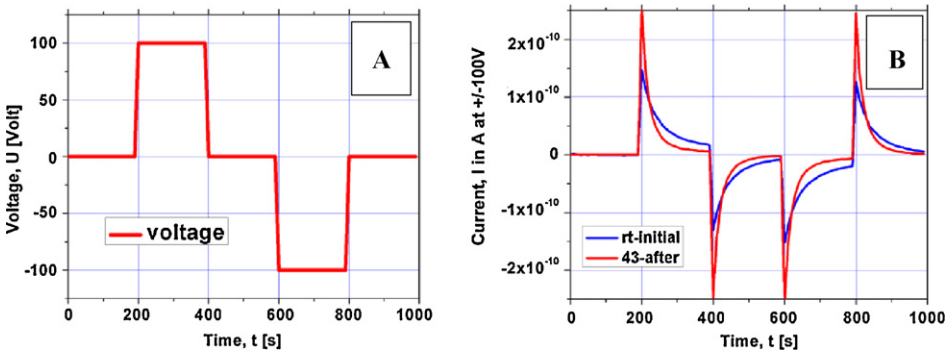

Fig. 1. Pulsed DC testing of Mn-doped TiO_2 sintered at 900 °C. (A) Applied voltage cyclogram at ±100 V. (B) Time dependence of measured current, blue curve – initial room temperature measurements without annealing; red curve – after heat treatment in dry air. (For interpretation of the references to color in this figure legend, the reader is referred to the web version of this article.)

Of particular interest in this investigation is the characterization of the Mn ion environment in nanostructured TiO_2 being considered for capacitors with high energy density. Besides high breakdown strength, such capacitors require high insulation resistance for efficient charge storage under applied electrical field. Whether the dopant becomes segregated at the grain boundaries or is uniformly distributed in the bulk will have a significant effect on electrical properties. Since the leakage current is closely related to dielectric breakdown phenomenon and the dielectric loss (particularly at low frequencies), reduction of electrical conductivity is of critical importance for successful application of dielectric materials in high-energy density capacitors.

2. Experimental

High purity TiO_2 powders (Toho Titanium Co. Ltd., Chigasaki, Japan) were used as starting material [11]. Manganese (II) acetate tetrahydrate (99.99%, Sigma–Aldrich, St. Louis, MO) was used for doping of TiO_2 powders with 0.05 mol% Mn. A stock solution of Mn precursor was prepared with high-purity anhydrate ethanol (99.5%, Sigma–Aldrich) as the solvent. TiO_2 powders were mixed with the stock solution followed by ball milling of the slurry for 12 h and dried under constant stirring on a hot plate. After grinding with mortar and pestle, doped powders were first uniaxially pressed at 50 MPa followed by cold isostatically pressing at 300 MPa. Disc-shaped samples were sintered in oxygen atmosphere at 900 °C and 1100 °C for 2 h. Microstructural characterization of Mn-doped TiO_2 samples by scanning electron microscopy (SEM) are reported elsewhere [11], and additional SEM images as a function of thermal treatment are presented herein, using the methods previously described [11].

Impedance data were collected at 550 °C with an impedance analyzer (Solartron 1260 Hampshire, UK) connected with Solartron 1296 dielectric interface, and analyzed using Zview software. Experimental data are normalized to the sample geometry and equivalent circuit used for fitting of the results. Direct current measurements were performed by a Keithley electrometer 6517A using voltage pulses ±100 V. Data shown in Fig. 1 were obtained at room temperature using a pulsed cyclogram for applied voltage (A) and current response to this cyclogram (B). All measurements were done in the temperature range from 200 °C to 550 °C so that conductivity of the material is sufficiently high to obtain a grain and grain boundary response from the impedance spectra. To minimize the surface conductivity of the samples due to humidity in the ambient air, DC measurements were conducted after heating of the samples to 200 °C and cooling to room temperature in a chamber with dry air atmosphere.

EPR measurements were performed on a Bruker EMX spectrometer at room temperature (296 °K) and 77 °K on powdered samples. First-derivative spectra were obtained with 100 kHz field modulation, with 3.0 G amplitude. Quartz EPR tubes of 4 mm diameter were filled with about 1.5 cm of material height at room temperature and 0.75 cm of material height at 77 °K with comparable packing density, and the EPR intensity data were normalized. The measurements at room temperature were taken at 9.81 GHz and at 77 °K at 9.40 GHz, the difference in frequency being due to the glass-dewar LN_2 insert. Though measurements were performed at both temperatures, many of the most interesting features with adequate signal to noise in the TiO_2 samples were only observed at 77 °K and only those results will be described in detail.

3. Results and discussion

The 77 K EPR spectra of undoped and Mn-doped TiO_2 are depicted in Fig. 2. The undoped sample gives a spectrum indistinguishable from cavity background. There are no features commonly observed due to the presence of Fe impurities [12,13] nor is there a signal attributable to oxygen vacancies, indicating that the density of these impurities and defects is less than 10^{15} cm^{-3}. The Mn-doped sample annealed at 900 °C presents only a relatively weak and broad resonance. However if the Mn^{2+} ions were well dispersed in the structure one would expect a typical six-line pattern due to the hyperfine interaction associated with the spin-5/2 ^{55}Mn nucleus [10]. This result could be interpreted as the manganese ions not being uniformly incorporated into the TiO_2 structure, but rather clustered along the grain boundaries and therefore consistent with the impedance results.

In order to test this assertion, an EPR spectrum was also obtained for the same Mn-doped sample subjected to a post-anneal at

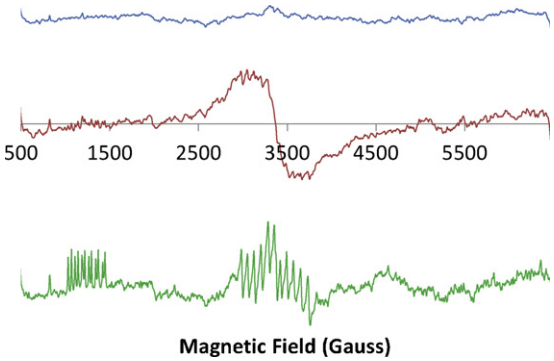

Fig. 2. 77 K EPR spectra of undoped (top), Mn-doped TiO_2 annealed at 900 °C (middle), Mn-doped TiO_2 annealed at 1100 °C (bottom).

1100 °C. In this case there are rich spectral features centered around 1250 G and 3300 G. Care was taken not to expose the sample to additional possible paramagnetic impurities during the post-anneal so it is believed that the principal effect of the higher temperature is to facilitate diffusion of the dopant ions throughout the bulk of the sample. The spectrum below is for the same sample subjected to a second annealing at 1100 °C, and shows multiple sites with clear hyperfine structure. The higher temperature annealing alters the distribution of the dopant ions to one that is more uniform throughout the bulk, which verifies our initial hypothesis that the 900 °C annealed sample has a non-uniform distribution of Mn ions. In the 1100 °C sample, there are two groups of g-values with 6 lines each overlapping. An essentially identical spectrum has been reported in Mn-doped TiO_2 and assigned to substitutionally incorporated Mn^{4+}, in which the fine structure term splits the multiplets into a double sextet resonance at 1000–1500 Gauss ($g \approx 4$) and another at around 3000 Gauss ($g \sim 2$) [14]. Despite the complexity of this spectrum, the main purpose here is to demonstrate that the lower temperature annealing process leaves the dopant ions segregated at the grain boundaries or otherwise clustered.

Because TiO_2 powders were doped by surface coating of the particles, clustering of Mn-ions at the grain boundaries occurs at low sintering temperatures. With the increase of sintering temperature, Mn-ions diffuse from the grain boundaries into the TiO_2 grains. The binding nature and preferential sites between Mn-ions and TiO_2 is governed by the interfacial reactions according to the phase equilibria in the MnO–TiO_2 system. The diffusion process during the initial stage of interfacial reactions may lead to formation of localized phases such as $MnTiO_3$, Mn_2TiO_4 or $MnTi_2O_5$ along the grain boundary region. Further increase of sintering temperature and time would result in diffusion of Mn-ions into the TiO_2 grains and dilution of dopant concentration within the grain boundaries. Further studies by utilizing of electron microscopy techniques are needed to reveal the nature and distribution of Mn- and Ti-ions along and near the grain boundaries of nanostructured TiO_2 dielectrics toward better understanding of the relationship between their electrical properties, microstructural evolution and defect structure. This point is addressed in greater detail later.

The effect of Mn doping on the dielectric properties of TiO_2 was reported in [11]. An optimized doping concentration of about 0.05 mol% led to reduced conductivity and loss tangent as well as improved voltage breakdown strength and energy storage capability of the dielectric due to generation of possible electron traps. Further increase of Mn content resulted in higher dielectric loss due to formation of oxygen vacancies. Increased grain-boundary resistivity was observed with higher Mn-doping concentration, presumably due to segregation of Mn solutes at the grain boundaries. Larger difference between the grain and grain-boundary conductivity gave rise to space charge polarization.

Comparison of impedance spectra for samples sintered at different temperatures is presented in Fig. 3. Cole–Cole plots (semicircles) shown in figure were measured at 550 °C and clearly represent two semicircles corresponding to grain and grain boundary resistance. While semicircles of 900 °C sample are less suppressed (more ideal), semicircles of 1100 °C sample are more suppressed that may be caused by Mn-ion diffusion from grain boundaries into the grains. A suppressed semicircle of impedance spectra indicates a non-uniform distribution of Mn-ions within the grains. Fitting experimental spectra by an equivalent circuit confirms this suggestion. A good fitting within the entire frequency range was achieved for the sample sintered at 900 °C. In contrast, the sample sintered at 1100 °C shows a distortion of both high and low frequency semicircles. In this case, the high and low frequency sections of the spectra are fitted separately to reveal formation of a diffusive layer of Mn-ions as a "core–shell" structure within the TiO_2 grains. The corresponding parameters of the impedance spectra and fitting errors are given in Table 1 for both samples. Reduction of the conductivity is of critical importance for successful application of dielectric materials in high energy density capacitors, since conductivity is closely related to dielectric breakdown phenomenon and dielectric loss (particularly at low frequencies). A decrease in conductivity by appropriate amount of Mn doping is attributed to creation of electron traps due to the fact that Mn^{4+} and Mn^{3+} have higher tendency for reduction as compared to Ti^{4+} in dielectric ceramics such as $BaTiO_3$ [15]. However, excessive doping of TiO_2 with Mn ions would result in a decrease of resistivity by

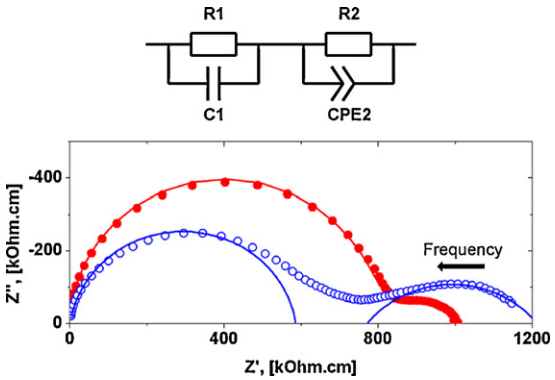

Fig. 3. Impedance spectroscopy of Mn-doped TiO_2 sintered at 900 °C (solid dots) and 1100 °C (open circles), data obtained at 550 °C. The lines are fitting curves obtained using the equivalent circuit.

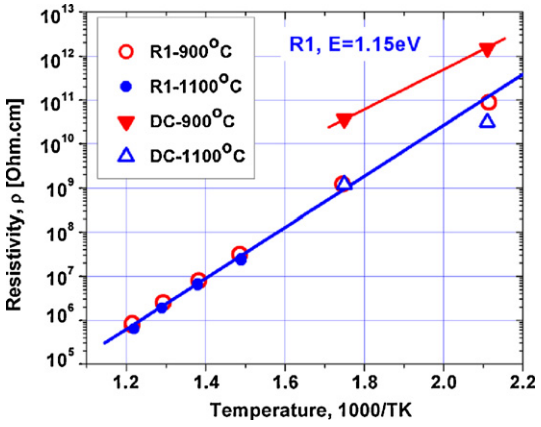

Fig. 4. Temperature dependence of resistivity for Mn-doped TiO_2 sintered at 900 °C (red signs) and 1100 °C (blue signs). Grain resistivities (circles) and total resistivities were measured by impedance spectroscopy and DC method, respectively. (For interpretation of the references to color in this figure legend, the reader is referred to the web version of this article.)

Table 1
Fitting results for impedance spectra (Fig. 1) obtained at 550 °C. For the sample sintered at 900 °C, the entire frequency range is fitted using an equivalent circuit. Two separate fittings were used for the sample sintered at 1100 °C: R1-C1 in the high frequency range and R2-CPE2 in the low frequency range.

Sintering temp. [°C]	R1 [Ohm]	C1 [F]	R2 [Ohm]	CPE2 [F]
900	8.4e5 ± 0.3%	8.0e-12 ± 0.25%	2.7e5 ± 1.2%	2.8e-9 ± 3.8%
1100	6.0e5 ± 1.5%	1.0e-11 ± 1.0%	4.5e5 ± 0.7%	4.3e-8 ± 2.7%

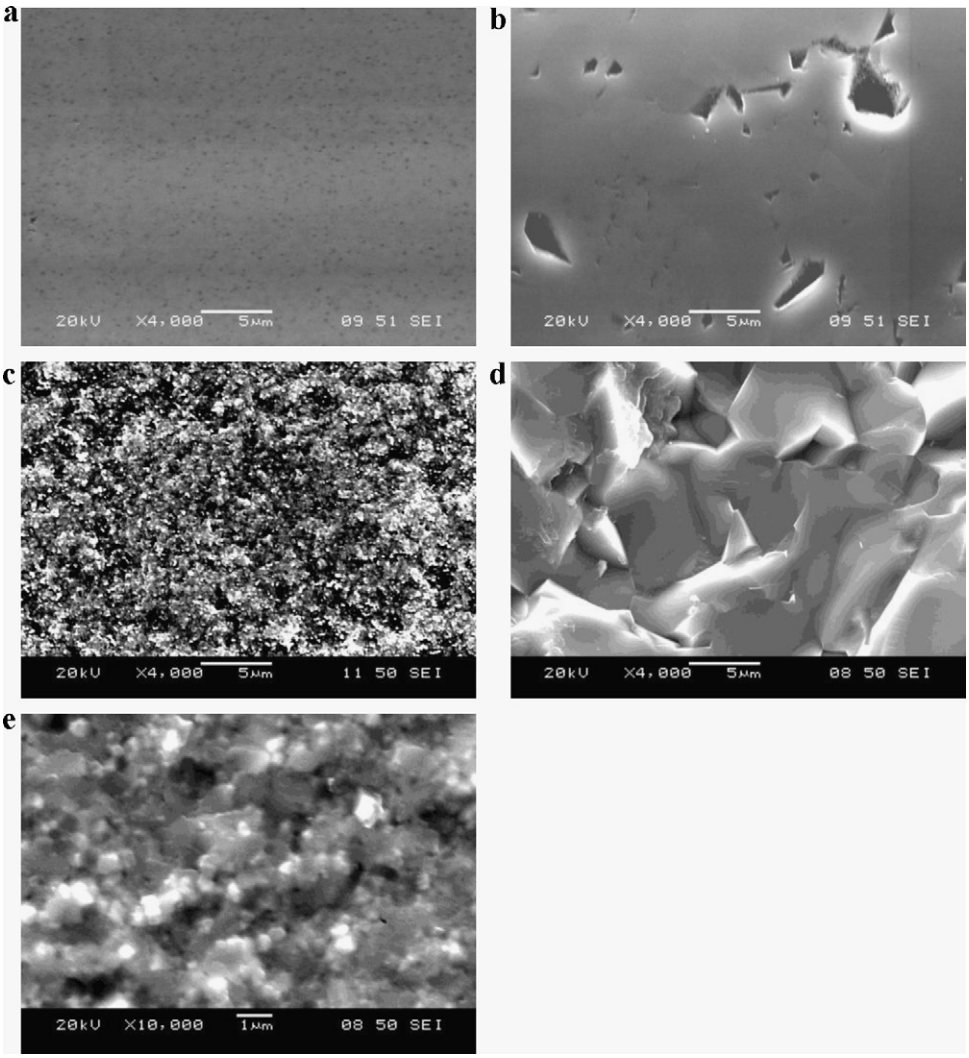

Fig. 5. SEM microstructural development of Mn-doped TiO_2 samples sintered at 900 °C and 1100 °C showing polished and fracture surfaces. (a) 900 °C polished; (b) 1100 °C polished; (c) 900 °C fracture; (d) 1100 °C fracture; (e) 900 °C fracture. Scale bar is 5 μm in (a)–(d), 1 μm in (e).

formation of oxygen vacancies that can be expressed by the following equations:

$$Mn_{Ti}^{X} + e' \leftrightarrow Mn_{Ti}' \quad (1)$$

$$Mn_{Ti}' + e' \leftrightarrow Mn_{Ti}'' \quad (2)$$

$$MnO \rightarrow Mn_{Ti}'' + V_O^{\bullet} + O_O^{X} \quad (3)$$

Fig. 4 shows the final results of electrical testing and includes temperature dependence of grain resistivity (R1) calculated from impedance spectra and DC resistivity measurements. Grain resistivity values for both samples are nearly the same with activation energy of 1.15 eV. DC resistivity of 1100 °C sample is nearly the same as R1 indicating that the impact of grain boundaries on overall resistivity of the sample is rather small. On the contrary, there is a significant (almost two orders of magnitude) difference between the grain and DC resistivity of 900 °C sample, i.e. grain boundary resistivity dominates overall resistivity of the sample. Hence, low temperature sintering of TiO_2 is necessary to prevent the diffusion of Mn-ions from the grain boundaries into the grains while densification of the dielectric is achieved. Sintering at higher temperatures leads to diffusion of Mn-ions into the grains and diffusion of Ti-ions into the grain boundaries that are initially occupied by Mn-ions.

Finally, microstructural development of Mn-doped TiO_2 samples sintered at 900 °C and 1100 °C are shown in the SEM images in Fig. 5. Polished and fracture surfaces of the samples reveal the differences between their grain size and the residual porosity. The average grain size of the samples sintered at 900 °C and 1100 °C are ~300 nm and 5 μm, respectively. Because the Mn-doping concentration (0.05 mol%) in TiO_2 was very low, the distribution of Mn-ions along and near the grain boundaries could not be resolved by SEM techniques. Further studies by utilizing transmission electron microscopy (TEM) techniques could possibly reveal the nature and distribution of Mn- and Ti-ions along and near the grain boundaries of nanostructured TiO_2 dielectrics, perhaps resulting in a better understanding of the relationship between their electrical properties, microstructural evolution and defect structure.

EPR, SEM, and electrical results of this study support the conclusions in Ref. [11] that low temperature sintering of Mn-doped TiO_2 leads to a dielectric material with improved insulation resistance suitable for development of high energy density ceramic capacitors. Higher grain boundary resistance is attributed to the smaller grain size and the segregation of dopants at the grain boundaries of Mn-doped TiO_2 sintered at lower temperatures (900 °C). Hence, we propose that both effects (grain boundary composition and grain size) are comparably important to obtain a lower leakage current in TiO_2 as a dielectric material for enhanced energy density capacitor applications.

4. Summary

The effect of sintering temperature on Mn-doped nanostructured TiO_2 dielectrics was studied by impedance spectroscopy, DC measurements and electron paramagnetic resonance techniques. It is shown that the insulation resistance of the sample sintered at 900 °C was higher than that of the sample sintered at 1100 °C. Impedance spectroscopy revealed that the grain boundary resistance of 900 °C sample with smaller grain size was significantly higher as compared to the 1100 °C sample while resistivities of grains were similar for both samples. EPR studies confirmed that improvement of insulation resistance is correlated with a non-uniform distribution of dopant ions, concentrated at the grain boundaries.

Acknowledgements

This work was supported by the U.S. Office of Naval Research. Hunter College acknowledges an infrastructure grant from the National Institutes of Health (RR 003037).

References

[1] M.-J. Pan, C.A. Randall, IEEE Electr. Insul. Mag. 26 (2010) 44.
[2] Y. Ye, S.Z. Zhang, F. Dogan, E. Schamiloglu, J. Gaudet, P. Castro, M. Roybal, M. Joler, C. Christodulou, 14th IEEE International Pulsed Power Conference, Dallas, TX, 2003, p. 719.
[3] S. Chao, V. Petrovsky, F. Dogan, J. Am. Ceram. Soc. 93 (2010) 3031.
[4] S. Chao, V. Petrovsky, F. Dogan, J. Mater. Sci. 45 (2010) 6685.
[5] D.W. Hahna, Y.H. Han, Ceram. Int. 34 (2008) 1341.
[6] Y. Takezawa, K. Kobayashi, F. Nakasone, T. Suzuki, Y. Mizuno, H. Imai, J. Appl. Phys. 48 (2009) 111408.
[7] A. Templeton, X. Wang, S.J. Penn, S.J. Webb, L.F. Cohen, N.M. Alford, J. Am. Ceram. Soc. 83 (2000) 95.
[8] M. Aono, R.R. Hasiguti, Phys. Rev. B 48 (1993) 17.
[9] S.T. Martin, C.L. Morrison, M.R. Hoffmann, J. Phys. Chem. 98 (1994) 13695.
[10] S. Güler, B. Rameev, R.I. Khaibullin, O.N. Lopatin, B. Aktaş, J. Phys.: Conf. Ser. 153 (2009) 12052.
[11] S. Chao, F. Dogan, J. Am. Ceram. Soc. 94 (2011) 179.
[12] P.-O. Anderson, E.L. Kollberg, Phys. Rev. B 8 (1973) 11.
[13] T. Tong, J. Zhang, B. Tian, F. Chen, D. He, J. Hazard. Mater. 155 (2008) 572.
[14] T.J. Kemp, R.A. McIntyre, Polym. Degrad. Stab. 91 (2006) 165.
[15] I. Burn, J. Mater. Sci. 14 (1979) 2453.